J. Phys.: Condens. Matter **20** (2008) 285223 (4pp) doi:10.1088/0953-8984/20/28/285223

Thermoelectric power studies on $(1 - x)$ $Pr_{2/3}Ba_{1/3}MnO_3 + x\,Ag_2O$ composites

Neeraj Panwar[1,2], D K Pandya[2] and S K Agarwal[1,3]

[1] Superconductivity and Cryogenics Division, National Physical Laboratory, Dr K S Krishnan Road, New Delhi-110012, India
[2] Department of Physics, Indian Institute of Technology, New Delhi-110016, India

E-mail: prof.agarwal@gmail.com

Received 21 April 2008, in final form 30 May 2008
Published 24 June 2008
Online at stacks.iop.org/JPhysCM/20/285223

Abstract

Thermoelectric power (TEP) measurements of $Pr_{2/3}Ba_{1/3}MnO_3 + Ag_2O$ composite manganites are reported here. A phase transition from metallic to insulating behaviour is observed for all the synthesized samples. No change in the TEP behaviour of the pristine sample $Pr_{2/3}Ba_{1/3}MnO_3$ is observed with Ag_2O addition. The phase transition temperature ($T_S \sim 196$ K) also does not change with Ag_2O which indicates the presence of Ag at the grain boundaries. In the insulating region TEP is large and negative, while in the metallic region it is positive with small values. The observed crossover from hole- to electron-like transport is attributed to the excitation of the valence band electrons to the conduction band with increasing temperature. The metallic region is found to be governed by the electron–magnon scattering process whereas a non-adiabatic small polaron hopping model is found applicable in the insulating regime.

1. Introduction

The discovery of the colossal magnetoresistance (CMR) effect in perovskite manganites during the last decade has gained much attention because of the potential applications of such materials for read heads of magnetic memory devices, magnetic field sensors and infrared bolometers etc [1–7]. High room temperature MR at low magnetic field is one of the stringent requirements of these devices. At the same time, a low electrical resistivity is also needed due to the circuit matching requirements. For this purpose composites of these manganites materials with non-metallic and metallic oxide phases have been reported [8–17]. Non-metallic oxide composites, however, increase the electrical resistivity of the pristine compound of the composites and shift the insulator–metal (I–M) transition towards lower temperatures (although with higher MR values) [8, 10, 11]. Lower resistivity values are obtained by making the grain boundaries of the manganites conducting. For this purpose conducting elements like Ag or Pd are found to be good choices because of their high electrical conductivity. More recently, we reported electrical resistivity, magnetotransport and magnetization studies of $Pr_{2/3}Ba_{1/3}MnO_3$ (PBMO) + Ag_2O wherein the MR of the pristine sample increases substantially with Ag also with an increase in conductivity [18]. In the electrical resistivity measurement of the pristine sample PBMO two insulator–metal (I–M) transitions are observed (at $T_{P1} \sim 194$ K and $T_{P2} \sim 160$ K). The higher temperature transition T_{P1} is ascribed to the competition between super-exchange and double-exchange mechanisms whereas the low temperature broad transition T_{P2} results from grain boundary effects that in turn correspond to the large ionic size mismatch between the ions present at the rare-earth site namely Pr^{+3} (1.18 Å) and Ba^{+2} (1.47 Å). With Ag_2O addition, the lower temperature transition is suppressed, whereas the high temperature transition at T_{P1} remains invariant but becomes sharper. On the other hand, in the magnetic measurements only a single paramagnetic–ferromagnetic (PM–FM) transition is observed at $T_C \sim 194$ K that matches with the I–M transition temperature T_{P1} [18]. Further, to know the appropriate mechanisms operating in different temperature regimes one needs to carry out the thermal measurements such as thermoelectric power, $S(T)$. Comparison of the electrical and thermal properties might confirm the type of carriers for the insulating/metallic behaviour of the manganites and also how the conduction of these carriers is governed i.e. through adiabatic or non-adiabatic process. We have therefore carried out thermoelectric power measurements on

[3] Author to whom any correspondence should be addressed.

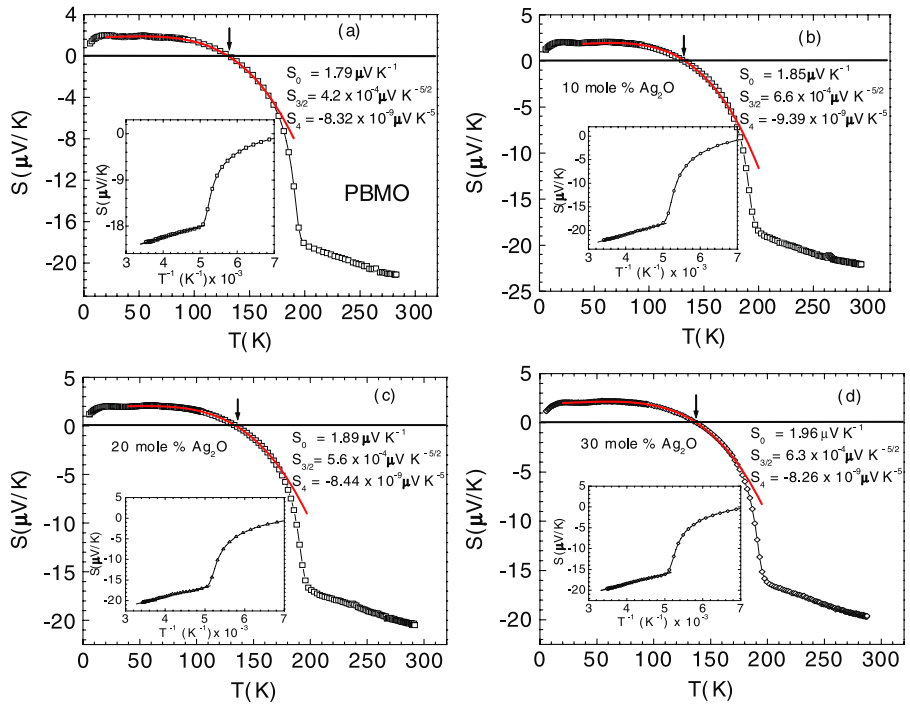

Figure 1. ((a)–(d)) Thermoelectric power of the composite manganites. Solid lines show the fitting using equation (3) whereas insets show the fitting above T_S with equation (1). The values of the fitted parameters of equation (3) are also shown.
(This figure is in colour only in the electronic version)

PBMO + Ag_2O composite manganites and explored various mechanisms operating in different temperature regimes. It is known that $S(T)$ measurement is sensitive to the nature of charge carriers and also is less affected by some factors like the presence of the grain boundaries, which often complicate the electrical resistivity measurements for the polycrystalline samples. Therefore, $S(T)$ should reflect the intrinsic properties of the samples. Hence, the transport mechanism should turn out to be more appropriate by the fitting of the $S(T)$ curve than by the electrical resistivity measurements.

2. Experimental details

Polycrystalline composites $(1-x)\,Pr_{2/3}Ba_{1/3}MnO_3 + x\,Ag_2O$ (where $x = 0$, 10, 20, 30 mol%) were synthesized using the conventional solid-state reaction method. The detailed synthesis procedure has already been explained elsewhere [18]. It is worth mentioning here that due to a low dissociation temperature (350 °C) of Ag_2O, it gets converted into metallic Ag during the synthesis process. Thermoelectric power (TEP) measurements were carried out by DC differential techniques over a temperature range of 5–300 K, with a temperature gradient of ∼1 K maintained throughout.

3. Results and discussion

Figures 1(a)–(d) depict the temperature dependence of thermoelectric power for the various $(1-x)\,Pr_{2/3}Ba_{1/3}MnO_3 + x\,Ag_2O$ composites. The nature of the curves is identical for all the samples (because of the absence of the masked grain boundary effects). Large negative S at high temperatures ($|S|$ is larger than 20 $\mu V\,K^{-1}$) and small positive S at low temperatures are reminiscent of the insulating and metallic characters respectively. With decreasing temperature the magnitude of S decreases slowly up to a temperature $T_S \sim 196$ K. Below T_S, S drops sharply signifying the occurrence of a phase transition from the high temperature insulating to low temperature metallic state. It is noted that T_S is very close to the insulator–metal transition temperature ($T_{P1} \sim 194$ K) of the electrical resistivity [18]. A crossover (indicated by a vertical downward arrow) from electron- to hole-like conduction is also noticed near 135 K (T^*) which can be attributed to the enhanced spin polarization with a decrease in temperature. S being very sensitive to the changes in the electronic structure, such a sign reversal in addition to the nature of charge carriers, indicates that there may be a substantial change in the band structure. Asamitsu *et al* [19] have shown a systematic variation of thermoelectric power with temperature in terms of change of the electronic structure with band filling and spin polarization in manganites. The above phenomenology is based on the vanishing of the exchange interaction, which arises due to the excitation of the electrons from the valence band (VB) t_{2g} to the conduction band (CB) e_g. The mobility of the electrons in the conduction band is high, leading to a negative thermoelectric power. The degeneracy of the e_g band seems to be gradually lifted as the temperature is lowered below T^* and the thermoelectric power changes its sign from negative to positive with the increase of spin polarization. With lowering of temperature below T^*, a broad hump in $S(T)$ is also observed.

We now turn to explore various mechanisms governing the thermoelectric power at different temperatures. It is worthwhile mentioning that the effect of Jahn–Teller distortion in manganites results in strong electron–phonon coupling and hence the formation of polarons [20]. Therefore, charge carriers in the insulating region above T_S are not itinerant and transport properties are governed by thermally activated carriers (polarons). We, therefore, fitted the $S(T)$ data above T_S (insets of figures 1(a)–(d)) with the Mott's polaron hopping relation [20]:

$$S(T) = \frac{k_B}{e}\left[\frac{E_S}{k_B T} + \alpha\right] \quad (1)$$

where k_B is the Boltzmann constant, e is the electronic charge, E_S is the activation energy required to activate the hopping of carriers and the constant α is related to the kinetic energy of the polarons [21]. $\alpha < 1$ suggests the conduction is due to small polarons hopping (SPH) whereas $\alpha > 2$ corresponds to the case of large polaron hopping (LPH) [20]. The value of E_S being very small (2.1 meV for pristine) and α less than 1 (α varies from -0.332 for PBMO to -0.329 for 30 mol% Ag_2O sample) confirm the carrier conduction through the hopping of small polarons in the insulating region.

Electrical resistivity, according to the polaron hopping model varies as $\rho = \rho_0 T^n \exp(\frac{E_\rho}{k_B T})$ [22], where $\rho_0 = [k_B/\nu_{ph} N e^2 R^2 C(1-C)]\exp(2\alpha R)$, n is 1 for adiabatic and 1.5 for non-adiabatic processes, N is the number of ion sites per unit volume (obtained from density data), R is the average intersite spacing given by $R = (1/N)^3$, C is the fraction of sites occupied by a polaron, α is the electron wavefunction decay constant, ν_{ph} is the optical phonon frequency (estimated from the relation $h\nu_{ph} = k_B\theta_D$, θ_D is the Debye temperature) and E_ρ is the sum of the activation energy required for the creation of carriers and activating the hopping of the carriers. In the adiabatic case, the hopping sites are near enough for the charge carrier to tunnel back and forth several times from one site to the other during one excited state of the system. On the other hand, in the non-adiabatic case, although the motion of the polaron in its well is adiabatic, the chance of the carrier tunnelling between adjacent sites during an excited state is small. We estimated E_ρ for each sample from the ln $(\rho/T^{1.5})$ versus $1/T$ plot. It varies from 152.06 meV for the PBMO sample to 134.25 meV for the 30 mol% Ag_2O added sample. Here $E_\rho > E_S$ indicates the applicability of the small polaron hopping model (their difference W_H is the polaron hopping energy). We further confirm the non-adiabatic conduction of small polarons by using the Holstein relation [23], which states that polaron bandwidth $J(T)$ should fulfil the criteria $J(T) < H$, where $H = (2k_B T W_H/\pi)^{1/4}(h\nu_{ph}/\pi)^{1/2}$ and evaluation of $J(T)$ can be made from the relation

$$J(T) \approx 0.67 h\nu_{ph}(T/\theta_D)^{1/4}. \quad (2)$$

For these composites H varies from 22.87 to 22.25 meV (calculated at an arbitrary temperature 250 K) and J (250 K) $\sim$ 21.27 meV (θ_D and ν_{ph} are 420 K and 8.78×10^{12} Hz, respectively, in the present case). Since $J(T) < H$, we can conclude that small polaron hopping conduction is a non-adiabatic process.

In the metallic region charge carriers from the Jahn–Teller polarons get delocalized and this may cause a significant amount of carrier–magnon scattering. To verify the above argument we attempted to fit the measured $S(T)$ data in the metallic region using the following relation [24, 25]:

$$S(T) = S_0 + S_{3/2}T^{3/2} + S_4 T^4, \quad (3)$$

where S_0 (value of S at $T = 0$ K) is inserted to account for the problem of truncating the low temperature data and a $T^{3/2}$ dependence is attributed to electron–magnon scattering process. The origin of the term S_4T^4, dominant in the high temperature region is still not clear but it has been conjectured to arise from the spin wave fluctuations in the ferromagnetic metallic (FMM) phase [24]. The quality of the fitting is given by the square of the linear correlation coefficient (R^2) and is nearly 99.9% for thermoelectric power data fitting. The solid lines show the fitting in figure 1 and the fitting parameters are in good accord with the reported data [24, 25]. It is clear that $S_{3/2}$ is nearly five orders of magnitude larger than S_4, implying the dominance of second term of equation (3). This confirms that the electron–magnon scattering process governs the metallic region of TEP below T_S.

4. Conclusions

Thermoelectric power measurements carried out on $Pr_{2/3}Ba_{1/3}MnO_3 + Ag_2O$ composite manganites exhibit no change in the behaviour from the pristine sample. As with the electrical resistivity, a transition from high temperature insulating to low temperature metallic behaviour has been observed for all the samples. The transition temperature also does not change with addition of Ag_2O, which indicates the presence of Ag at the grain boundaries. The observed crossover from hole- to electron-like transport is attributed to the excitation of the valence band electrons to the conduction band with increasing temperature. The metallic region is found obey the electron–magnon scattering process whereas the non-adiabatic small polaron hopping model governs the insulating regime.

Acknowledgments

The authors thank the Director, National Physical Laboratory, New Delhi, for his support and interest in the present work. The authors also thank Professor Ajay Gupta, Center Director and Dr V Ganesan of the UGC-DAE Consortium for Scientific Research, Indore, for their support for thermal measurements. One of the authors (NP) would like to thank CSIR, India, for the grant of a Senior Research Fellowship.

References

[1] von Helmolt R, Wacker J, Holzapfel B, Schultz M and Samwer K 1993 *Phys. Rev. Lett.* **71** 2331
[2] Jin S, Tiefel T H, McCormack M, Fastnacht R A, Ramesh R and Chen L H 1994 *Science* **264** 413
[3] Kuwahara H, Tomioka Y, Asamitsu A, Moritomo Y and Tokura Y 1995 *Science* **270** 961
[4] Obata T, Manako T, Shimakawa Y and Kubo Y 1999 *Appl. Phys. Lett.* **74** 290

[5] Li X W, Lu Y, Gong G Q, Xiao G, Gupta A, Lecoeur P, Sun J Z, Wang Y Y and Dravid V P 1997 *J. Appl. Phys.* **81** 5509
[6] Prinz G 1995 *Phys. Today* **48** 58
[7] Rajeswari M, Chen C H, Goyal A, Kwon C, Robson M C, Ramesh R, Venkatesan T and Lakeou S 1996 *Appl. Phys. Lett.* **68** 3555
[8] Karmakar S, Taran S, Chaudhuri B K, Sakata H, Sun C P, Huang C L and Yang H D 2005 *J. Phys. D: Appl. Phys.* **38** 3757
[9] Moshnyaga V, Damaschke B, Shapoval O, Belenchuk A, Faupel J, Lebedev O I, Verbeeck J, Tendeloo G V, Mücksch M, Tsurkan V, Tidecks R and Samwer K 2003 *Nat. Mater.* **2** 247
[10] Gaur A, Varma G D and Singh H K 2006 *J. Phys. D: Appl. Phys.* **39** 3531
[11] Kang B S, Wang H, MacManus-Driscoll J L, Li Y, Jia Q X, Mihut I and Betts J B 2006 *Appl. Phys. Lett.* **88** 192514
[12] Zhang N and Wang M 2006 *Appl. Phys. Lett.* **88** 122111
[13] Yao L D, Zhang W, Zhang J S, Yang H, Li F Y, Liu Z X, Jin C Q and Yu R C 2007 *J. Appl. Phys.* **101** 063905
[14] Miao J-H, Yuan S-L, Ren G-M, Xiao X, Yu G-Q, Wang Y-Q and Yin S-Y 2006 *J. Phys. D: Appl. Phys.* **39** 2897
[15] Pal S, Banerjee A, Chaterjee S, Nigam A K, Chaudhuri B K and Yang H D 2003 *J. Appl. Phys.* **94** 3485
[16] Yuan X-B, Liu Y-H, Wang C-J and Mei L-M 2006 *Appl. Phys. Lett.* **88** 042508
[17] Yuan X-B, Liu Y-H, Yin N, Wang C-J and Mei L-M 2006 *J. Phys. D: Appl. Phys.* **39** 1028
[18] Panwar N, Pandya D K and Agarwal S K 2007 *J. Phys.: Condens. Matter* **19** 456224
[19] Asamitsu A, Moritomo Y and Tokura Y 1996 *Phys. Rev.* B **53** R2952
[20] Mott N F and Davis E A (ed) 1979 *Electronic Processes in Non-Crystalline Materials* (Oxford: Clarendon)
[21] Sega K, Kuroda Y and Sakata H 1998 *J. Mater. Sci.* **33** 1303
[22] Emin D and Holstein T 1969 *Ann. Phys.* **53** 439
[23] Holstein T 1959 *Ann. Phys.* **8** 343
[24] Banerjee A, Pal S, Bhattacharya S, Chaudhuri B K and Yang H D 2001 *Phys. Rev.* B **64** 104428
[25] Mandal P 2000 *Phys. Rev.* B **61** 14675